

Published in final edited form as:

*Nat Immunol.* 2014 September ; 15(9): 875–883. doi:10.1038/ni.2958.

## The tyrosine phosphatase Ptpn22 discriminates weak, self-peptide from strong agonist T cell receptor signals

Robert J. Salmond<sup>#1</sup>, Rebecca J. Brownlie<sup>#1</sup>, Vicky L. Morrison<sup>2</sup>, and Rose Zamoyska<sup>1,\*</sup>

<sup>1</sup>Institute of Immunology and Infection Research, Centre for Immunity, Infection and Evolution, Ashworth Laboratories, The King's Buildings, University of Edinburgh, West Mains Road, Edinburgh, EH9 3JT, UK

<sup>2</sup>Medical Research Institute, Ninewells Hospital and Medical School, University of Dundee, Dundee, DD1 9SY, UK

# These authors contributed equally to this work.

### Abstract

T cells must be tolerant of self-antigens to avoid autoimmunity, but responsive to foreign-antigens to provide protection against infection. We found that in both naive and effector T cells, the tyrosine phosphatase, Ptpn22 limits T cell receptor signaling by weak agonist and self-antigens, while not impeding responses to strong agonist antigens. T cells lacking Ptpn22 show enhanced conjugate formation with antigen presenting cells pulsed with weak peptides, leading to their activation and production of inflammatory cytokines. This effect is exacerbated under conditions of lymphopenia with the formation of potent memory T cells in the absence of Ptpn22. These data address how loss of function *PTPN22* alleles can lead to expansion of effector/memory T cells and a predisposition to human autoimmunity.

---

The maintenance of naive T cell tolerance requires the T cell receptor (TCR) signaling machinery to discriminate between low affinity self-peptide:MHC (pMHC) interactions, which provide survival but not activation signals in the periphery<sup>1</sup>, and signals from pathogen-derived peptides that stimulate effector T cell responses and the development of memory. Transient lymphopenia exacerbates this situation with stimulation by weak self-pMHC and interleukin-7 (IL-7) combining to drive slow homeostatic proliferation (HP) of naive T cells and their conversion to a memory phenotype<sup>2-4</sup>. Homeostatic expansion following lymphopenia has been linked to the development of autoimmunity in humans following infection<sup>4</sup>, immunosuppressive therapies<sup>5,6</sup> and in autoimmune prone NOD

---

Users may view, print, copy, and download text and data-mine the content in such documents, for the purposes of academic research, subject always to the full Conditions of use:[http://www.nature.com/authors/editorial\\_policies/license.html#terms](http://www.nature.com/authors/editorial_policies/license.html#terms)

\*Correspondence should be addressed to R.Z. (Rose.Zamoyska@ed.ac.uk), Telephone: +44 131 6513686 Fax: +44 131 650 6564.

#### Author contributions

R.J.S. designed and performed most *in vitro* experiments and co-wrote the manuscript. R.J.B. designed and performed most *in vivo* experiments and *in vitro* analyses of T cell conjugate formation. V.M. designed and performed analyses of adhesion under shear flow. R.Z. designed experiments, led the overall project and co-wrote the manuscript.

#### COMPETING FINANCIAL INTERESTS

The authors declare no competing financial interests.

mice<sup>7</sup>. In the latter study, NOD mice showed that transient lymphopenia combined with genetic predisposition precipitated autoimmune disease.

Amongst the genes identified in genome wide association studies (GWAS) that increase susceptibility to autoimmunity are hematopoietic phosphatases<sup>8</sup>. It has long been recognized that inhibitory tyrosine phosphatases dampen T cell responses and that generic phosphatase inhibitors induce T cell activation in the absence of TCR triggering, indicating that they function as gatekeepers, curbing T cell activation<sup>9</sup>. However, we lack a more general understanding of how specific phosphatases identified in GWAS screens influence the balance between tolerance and responsiveness in T cells, which is key to comprehending their involvement in predisposition to autoimmune diseases.

The cytoplasmic tyrosine phosphatase PTPN22 has attracted much attention as a significant risk allele for the development of numerous autoimmune diseases including rheumatoid arthritis (RA) and type 1 diabetes (T1D) (reviewed in<sup>10</sup>). *Ptpn22*-deficient mouse strains accumulate effector/memory phenotype T cells to a significantly greater extent than in wild type (WT) naive mice<sup>11,12</sup>. Two groups independently reported the generation of *Ptpn22* R619W knock-in (KI) mice, a model for a disease-associated *PTPN22* single-nucleotide polymorphism (SNP)<sup>13,14</sup>. Both reported a similar, albeit milder, effect of the KI mutation on T cell homeostasis as had been reported for knock-out mice, suggesting the SNP acts, in mice at least, as a loss-of-function allele. On a mixed genetic background the KI mice developed multiple features of autoimmunity<sup>13</sup>. These papers suggested that loss of expression or function of *Ptpn22* primarily impacts upon effector T cell activation, as naive T cell activation was unaffected. In both human and mouse with either *PTPN22* variants or *Ptpn22*<sup>-/-</sup> alleles there is expansion of effector/memory T cells. A key remaining question is: what drives the expansion of effector/memory T cells in the presence of loss-of-function *PTPN22* alleles and does this expansion contribute to loss of self-tolerance?

We show here that naive T cell responses are influenced by loss of *Ptpn22*. In OT-1 TCR transgenic T cells, *Ptpn22* is critical to limit the response to weak, but not strong, agonist peptides. In contrast to WT cells, naive *Ptpn22*<sup>-/-</sup> T cells expand more and acquire full effector function under conditions of lymphopenia. *Ptpn22*<sup>-/-</sup> CD8 cytotoxic T lymphocytes (CTLs) become potentially self-reactive, producing inflammatory cytokines in response to self-peptide. These data identify a vital role for *Ptpn22* in TCR ligand discrimination and provide an insight into the mechanism of action of this phosphatase in human disease.

## RESULTS

### ***Ptpn22*<sup>-/-</sup> T cells show elevated homeostatic proliferation**

Studies using mice with a polyclonal T cell repertoire have shown that, in the absence of *Ptpn22*, memory/effector phenotype T cells accumulate in secondary lymphoid tissues<sup>11,12</sup>. Whether the memory/effector cell expansion resulted from persistence of cells driven to respond by foreign/high affinity Ags or whether it stemmed from a loss of homeostatic regulation of naive T cells by self or low affinity Ags was not determined. The fact that enhanced signaling was only apparent in *Ptpn22*<sup>-/-</sup> effector and not naive T cells suggested

the former<sup>11,12</sup>. To determine the primary cause of T cell dysregulation in this model, we crossed *Ptpn22*<sup>-/-</sup> mice to the H-2Kb-restricted OT-1 TCR transgenic *Rag1*<sup>-/-</sup> mouse.

Comparisons of thymi from 7 wk old WT and *Ptpn22*<sup>-/-</sup> OT-1 mice showed that there was approximately a 40% reduction in the numbers of CD4<sup>+</sup>CD8<sup>+</sup> double-positive (DP) OT-1 thymocytes (Supplementary Fig. 1a-d). This may be linked to the premature expression of the OT-1 TCR as polyclonal *Ptpn22*<sup>-/-</sup> DP numbers were shown to be unaffected<sup>11,12</sup>, but this did not appear to impact on CD8 SP differentiation. Thus single-positive (SP) thymocyte subpopulations were equivalent both in terms of cell number (Supplementary Fig. 1d) and phenotype (data not shown). These data are consistent with findings suggesting that disease-associated PTPN22 variants do not impact upon negative selection<sup>15</sup>.

Numbers of CD8 T cells in LN of 7 wk old WT and *Ptpn22*<sup>-/-</sup> OT-1 mice were comparable (Fig. 1a). The expression of TCR, CD5, CD8, CD11a, and CD98 by flow cytometry were similar between the two genotypes (Supplementary Fig. 1e). Overall both WT and *Ptpn22*<sup>-/-</sup> OT-1 cells maintained a naive phenotype, uniformly expressing high amounts of CD62L and CD127 (IL-7R $\alpha$ ), and were negative for expression of the activation marker CD69 (Supplementary Fig. 1e). However, there were indications of elevated basal activation in the *Ptpn22*<sup>-/-</sup> OT-1 T cells. For example, Ki-67, a marker of proliferation, was expressed in a significantly higher proportion of *Ptpn22*<sup>-/-</sup> OT-1 T cells (Fig. 1b,c). The inflammatory chemokine receptor CXCR3 was expressed on 10-30% of *Ptpn22*<sup>-/-</sup> OT-1 T cells but only 3-7% of WT counterparts whereas CD44 expression was very slightly, but consistently, elevated on *Ptpn22*<sup>-/-</sup> cells (Fig. 1d,e). Flow cytometry of key transcription factors (TFs) showed a consistent, albeit modest, increase in T-bet and eomesodermin protein (Eomes) staining in *Ptpn22*<sup>-/-</sup> naive OT-1 T cells (Fig. 1f,g).

The OT-1 recombinase activating gene deficient (*Rag1*<sup>-/-</sup>) background is mildly lymphopenic due to the absence of B cells and CD4 T cells and we hypothesized that this might account for the signs of activation amongst the naive *Ptpn22*<sup>-/-</sup> OT-1 T cells. We reasoned that in a more profoundly lymphopenic setting this effect would be enhanced. Limited numbers of *Ptpn22*<sup>-/-</sup> CD45.2<sup>+</sup> and *Ptpn22*<sup>+/+</sup> CD45.1<sup>+</sup> OT-1 T cells were co-transferred into *Rag1*<sup>-/-</sup> hosts at a ~1:1 ratio (Fig. 2a). After 7 (data not shown) and 14 days (Fig. 2b) numbers of recovered donor cells were low and proportions of WT and *Ptpn22*<sup>-/-</sup> cells were equivalent, consistent with the slow HP that is driven by contact with self-ligands in a lymphopenic environment. At 4 weeks post transfer both WT and *Ptpn22*<sup>-/-</sup> cells had increased in number. At this time point significantly greater proportions (Fig. 2c) and numbers (Fig. 2d) of *Ptpn22*<sup>-/-</sup> cells were recovered.

Slow homeostatic proliferation under conditions of lymphopenia is driven by a combination of self-pMHC and IL-7. Typically the increased IL-7 availability in a lymphopenic environment amplifies the weak TCR signal<sup>16</sup>. In order to discriminate whether responsiveness to TCR stimulation or IL-7 was affected by loss of Ptpn22, we repeated the transfers and treated recipients with either PBS or anti-IL-7R monoclonal antibody (mAb) every 3 days. Fourteen days after transfer in the presence of anti-IL-7R mAb, significantly higher proportions of *Ptpn22*<sup>-/-</sup> cells had proliferated compared with WT cells (Fig. 2b). Although the total number of cells recovered from both WT and *Ptpn22*<sup>-/-</sup> genotypes was

reduced by 5-10 fold following IL-7R treatment, indicating that both cell types were similarly responsive to IL-7 survival signals, blockade of IL-7R clearly revealed weak TCR signals as the drivers of the increased responsiveness of *Ptpn22*<sup>-/-</sup> T cells.

To determine if this effect on T cell HP was a general feature of *Ptpn22*-deficiency, we used polyclonal CD4 T cells from two distinct *Ptpn22*<sup>-/-</sup> mouse strains. In germline *Ptpn22*<sup>-/-</sup> mice, *Ptpn22* is deleted in all cell types<sup>11</sup>, whereas in dLck-Cre mice, deletion of the LoxP-flanked allele occurs in post-positive selection thymocytes<sup>17</sup>. These experiments also address whether the behavior of *Ptpn22*<sup>-/-</sup> polyclonal T cells is due to alterations in thymic selection rather than an inherent difference in naive T cell responsiveness. We used sublethally irradiated WT recipients to avoid responses to gut antigens that can occur in *Rag1*<sup>-/-</sup> recipients, and so that we could measure proliferation of transferred polyclonal T cells preferentially in response to homeostatic cytokines and low affinity or self-Ag<sup>18</sup>. Naive CD44<sup>lo</sup> CD4 T cells from CD45.1<sup>+</sup> WT, CD45.2<sup>+</sup> *Ptpn22*<sup>-/-</sup> and GFP<sup>+</sup> dLck *Ptpn22*<sup>-/-</sup> mice were labeled with CellTrace Violet dye, mixed at ~1:1:1 ratio and transferred into irradiated recipients. After 14 days, donor cells were recovered. T cells from both *Ptpn22*-deficient strains were present in equal proportions and at significantly higher numbers than WT cells (Fig. 2e). Furthermore, flow cytometry showed that proportionally fewer WT cells had completely diluted cell tracer dye, indicative of slower rates of proliferation (Fig. 2f).

These data show that lymphopenia drives proliferation of naive *Ptpn22*<sup>-/-</sup> polyclonal and OT-1 T cells to a greater extent than WT T cells. The absence of cognate Ag and the slow rate of proliferation in the OT-1 model, together with the increased proliferation of *Ptpn22*<sup>-/-</sup> cells in the presence of IL-7R blockade, suggests that this expansion is driven by low-affinity and/or self pMHC.

### **Ptpn22 restrains TCR signaling induced by weak agonists**

We set out to test directly the hypothesis that Ptpn22 expression is essential for regulation of TCR responses to low affinity pMHC. A number of altered peptide ligands (APL) that vary in their potency to stimulate OT-1 thymocytes and T cells have been characterized<sup>19,20</sup>. We assessed the impact of *Ptpn22*-deficiency on naive T cell responses to 3 peptides: the agonist SIINFELK (N4), the partial agonist SIITFEKL (T4), and very weak agonist SIIGFEKL (G4). Of note, the T4 ligand is a threshold agonist for negative selection of OT-1 thymocytes; such ligands are thought to be particularly relevant for autoimmunity<sup>21,22</sup>.

To investigate early signals, WT CD45.1<sup>+</sup> *Rag1*<sup>-/-</sup> OT-1 and CD45.2<sup>+</sup> *Ptpn22*<sup>-/-</sup> *Rag1*<sup>-/-</sup> OT-1 cells were mixed 1:1, stimulated *in vitro* with N4, T4 or G4 peptides and levels of phospho-ERK (p-ERK) MAPK were measured by flow cytometry. Proportions of p-ERK<sup>+</sup> OT-1 cells were maximal by 15 mins of N4 stimulation, having reached a plateau, and the kinetics and magnitude of this response were equivalent for WT and *Ptpn22*<sup>-/-</sup> OT-1 cells (Fig. 3a). At these early time points, stimulation with either T4 or G4 peptides induced only a very low proportion of p-ERK<sup>+</sup> cells (Fig. 3a), consistent with reports that weaker agonists induce activation of MAPK with delayed kinetics<sup>20</sup>. At later time points, between 30 and 120 mins after T4 or G4 peptide stimulation, significantly ( $p < 0.05$ ) more *Ptpn22*<sup>-/-</sup> than WT OT-1 cells were p-ERK<sup>+</sup> (Fig. 3b,c). Furthermore, weak agonist-induced activation of

the kinase p90 ribosomal S6 kinase (RSK), which is downstream of ERK, was also significantly enhanced in the absence of Ptpn22 at these time points (Fig. 3b,d).

TCR-induced activation of the Ras-MAPK pathway is important for up-regulation of the early activation marker CD69<sup>23</sup>. As expected, 4h stimulation with the strong agonist N4 peptide induced high amounts of CD69 expression (Fig. 3e) with WT and *Ptpn22*<sup>-/-</sup> OT-1 cells responding similarly over a range of peptide concentrations (Fig. 3f). Consistent with their enhanced ERK phosphorylation naive *Ptpn22*<sup>-/-</sup> OT-1 cells were more responsive than WT cells to T4 and G4 peptide stimulation as indicated by a substantially higher proportion of CD69<sup>+</sup> cells (Fig. 3e,f). These data show that Ptpn22 suppresses early biochemical signals in response to TCR stimulation selectively to weak ligands, without decreasing the response to strong agonist ligand

TCR-induced expression of TFs regulates the fate of CD8 T cells (reviewed in<sup>24</sup>). Expression of T-bet<sup>25</sup> and Myc<sup>26</sup> is required for the differentiation of protective effector T cells, whereas expression of Eomes is associated with memory cell formation<sup>27</sup>. The induced expression of T-bet and Myc in both WT and *Ptpn22*<sup>-/-</sup> OT-1 was directly correlated with the strength of TCR signal received (N4>T4>G4). T-bet and Myc protein were more highly expressed in *Ptpn22*<sup>-/-</sup> T cells in response to all three peptide ligands, although Myc upregulation in response to the weakest stimulus, G4, did not reach significance (Fig. 4a and Supplementary Fig. 2a, b). In contrast, Eomes expression was inversely correlated with strength of signal (N4<T4<G4) and stimulation with N4 and T4 induced higher levels of Eomes expression in *Ptpn22*<sup>-/-</sup> OT-1 cells, whereas the weakest G4 peptide showed equivalent Eomes upregulation (Fig. 4a and Supplementary Fig. 2c). Therefore, the greatest difference in upregulation of memory-associated Eomes protein expression between *Ptpn22*<sup>-/-</sup> and WT cells is evident following strong agonist N4 stimulation, whereas for the other TFs it is particularly apparent following weak agonist stimulation.

The TF IRF4 has recently been linked to the preferential expansion and effector function of high affinity CD8 T cell clones<sup>28-30</sup>. IRF4 is upregulated proportionally to the strength of TCR signal while forced IRF4 expression facilitated expansion of CD8 T cells to lower affinity ligands<sup>28</sup>. In response to the weak ligands, T4 and G4, significantly higher protein expression of IRF4 was observed in *Ptpn22*<sup>-/-</sup> than in WT OT-1 cells (Fig. 4b and Supplementary Fig. 2d), whereas equivalent IRF4 upregulation occurred in response to the strong ligand, N4.

IRF4 was shown to regulate the majority of TCR-affinity driven transcriptional changes in CD8 T cells, including those genes required for key metabolic functions as the cells shift from oxidative phosphorylation to aerobic glycolysis in order to cope with the bioenergetics demands involved in proliferation and development of effector function<sup>28</sup>. In keeping with this we showed that when stimulated with weak agonist T4 and G4 peptides, *Ptpn22*<sup>-/-</sup> OT-1 cells were larger than WT cells, as indicated by increased forward scatter intensity, and had elevated glucose uptake (Fig. 4c and Supplementary Fig. 2e,f). In contrast, N4 stimulation of WT and *Ptpn22*<sup>-/-</sup> OT-1 T cells resulted in equivalent increases in both forward scatter and glucose uptake. Furthermore, 24h stimulation with weak agonists also

induced a higher amount of expression of the transferrin receptor CD71 protein (Supplementary Fig. 2g), but not the amino acid transporter CD98 (Supplementary Fig. 2h) by *Ptpn22*<sup>-/-</sup> OT-1 cells. These data are consistent with the higher upregulation of IRF4 in *Ptpn22*<sup>-/-</sup> T cells contributing to their preferential activation in response to weak ligands.

The impact of *Ptpn22*-deficiency on TCR-induced proliferation was assessed by dilution of CellTrace Violet dye. As has been reported for polyclonal T cells activated using CD3 and CD28 mAbs<sup>12</sup>, after 48h of peptide stimulation, *Ptpn22*<sup>-/-</sup> OT-1 cells proliferated to a greater extent than WT cells (Fig. 4d). Altogether these data indicate that, in naive WT T cells *Ptpn22* acts to restrain TCR-induced cell growth, metabolism, transcription factor expression and proliferation. For many parameters, these effects are most evident following weak rather than strong agonist stimulation and provide a basis for the observed expansion of effector/memory cells in the absence of *Ptpn22*.

### **Ptpn22 limits cytokines induced by weak agonists**

Thus far, our data implicated *Ptpn22* in the regulation of naive T cell responses to low affinity Ags with few differences in activation in response to high affinity Ags. Previous data had suggested that *Ptpn22* was particularly important in regulating effector T cell responses<sup>11,12</sup>, therefore we generated effector WT and *Ptpn22*<sup>-/-</sup> OT-1 CTLs and tested their recall responses to the variant peptides. For generation of CTLs *in vivo*, naive WT CD45.1+ and *Ptpn22*<sup>-/-</sup> CD45.2+ OT-1 cells were mixed 1:1, transferred to *Rag1*<sup>-/-</sup> recipient mice that were subsequently infected with an ova-expressing recombinant strain of *Listeria monocytogenes* (LmOva)<sup>31</sup>. On day 7, WT and *Ptpn22*<sup>-/-</sup> OT-1 cells in spleens were enumerated then re-stimulated *in vitro* with N4, T4 or G4 peptides for 4h. *Ptpn22*<sup>-/-</sup> OT-1 cells were present in significantly higher numbers following LmOva infection (Fig. 5a), indicating that *Ptpn22* negatively regulates infection-induced expansion of T cells *in vivo* in a lymphopenic environment. Furthermore, upon re-stimulation with weak agonist T4 and G4 peptides, significantly more *Ptpn22*<sup>-/-</sup> OT-1 cells produced the inflammatory cytokine IFN- $\gamma$ , whereas WT and *Ptpn22*<sup>-/-</sup> cells responded equally to the strong agonist N4 (Fig. 5b-d).

We then generated WT and *Ptpn22*<sup>-/-</sup> OT-1 CTLs *in vitro* by stimulation for 2d with N4 peptide, followed by 4d differentiation in the presence of a high dose of IL-2. The growth of CTLs in IL-2 was unaffected by *Ptpn22*-deficiency (Supplementary Fig. 3a), furthermore the size of WT and *Ptpn22*<sup>-/-</sup> CTLs and their surface expression of CD44, CD62L, CXCR3, CD27, CD25, CD127, CD132, KLRG1 and CD73 were similar (Supplementary Fig. 3b). Expression of the key TFs T-bet and Eomes and effector proteins granzyme B and perforin were comparable in both genotypes (Supplementary Fig. 3c), suggesting that differentiation of CTLs under these optimal *in vitro* conditions following stimulation with strong agonist was not overtly altered in the absence of *Ptpn22*. Nonetheless, re-stimulation revealed the same bias as before, with weak agonist T4 and G4 peptides, but not the strong agonist N4, stimulating substantially more *Ptpn22*<sup>-/-</sup> CTLs to produce IFN- $\gamma$  (Fig. 5e-g), the inflammatory cytokines TNF, GM-CSF and the inflammatory chemokine CCL3 (Supplementary Fig. 4).

Given the ability of weak Ags to stimulate responses from *Ptpn22*<sup>-/-</sup> naive T cells, we wished to determine whether *Ptpn22*<sup>-/-</sup> effector CTLs had the capacity to break tolerance *in vitro*. A peptide derived from  $\beta$ -catenin, RTYTYEKL, has been demonstrated to act as an endogenous positive-selecting ligand for OT-1 thymocytes, whereas mature, naive OT-1 T cells are completely unresponsive to this peptide<sup>32</sup>. OT-1 CTLs were generated as above and re-stimulated with RTYTYEKL. The response of *Ptpn22*<sup>-/-</sup> CTLs to the self-peptide was markedly elevated compared to WT CTL with a 5-fold and 3-fold increase in cells producing IFN- $\gamma$  and TNF, respectively (Fig. 5h,i). Finally, we tested the recall responses of CTLs grown *in vitro* under less inflammatory conditions, that is, differentiated in the presence of IL-15. Under these conditions WT CTLs were unresponsive to re-stimulation with the RTYTYEKL self-peptide, whereas a small but clearly detectable proportion of *Ptpn22*<sup>-/-</sup> cells responded by producing IFN- $\gamma$  (Fig. 5j). Together these data indicate that, in effector CTLs, Ptpn22 is critical for regulating TCR sensitivity and deficiency of Ptpn22 becomes permissive for the production of an inflammatory response to self-Ag.

### HP-induced *Ptpn22*<sup>-/-</sup> memory T cells are more inflammatory

Having determined an important role for Ptpn22 in TCR ligand discrimination in both naive and effector CD8 T cells, we addressed the role of the phosphatase in memory cells. Naive CD45-congenic WT and *Ptpn22*<sup>-/-</sup> OT-1 T cells were mixed 1:1 and transferred to *Rag1*<sup>-/-</sup> recipients which were either infected with LmOva or left uninfected. After 30d, both WT and *Ptpn22*<sup>-/-</sup> cells were predominantly of a CD44<sup>hi</sup> memory phenotype, with similar protein expression of CD62L, KLRG1 and CD127, irrespective of LmOva infection (data not shown). Within uninfected controls in which the cells had expanded in response to lymphopenia only, more *Ptpn22*<sup>-/-</sup> than WT OT-1 cells produced IFN- $\gamma$  upon re-stimulation with all peptides *in vitro* (Fig. 6a-c) and this was particularly striking upon re-stimulation with the weaker ligands, T4 and G4. *Ptpn22*<sup>-/-</sup> memory cells induced by infection with strong agonist LmOva had elevated IFN- $\gamma$  recall responses to T4 that were statistically significant, although this difference was rather small compared to those observed between WT and *Ptpn22*<sup>-/-</sup> naive and effector CD8 T cells. Furthermore, recall responses of LmOva-induced WT and *Ptpn22*<sup>-/-</sup> memory cells to N4 and G4 peptides were equivalent (Fig. 6d-f). Of note, in the *Rag1*<sup>-/-</sup> hosts, lack of competition from endogenous cells reduces contraction of the antigen-specific effector cells following pathogen elimination in the lymphopenic host. Therefore, the quality of the LmOva-induced WT and *Ptpn22*<sup>-/-</sup> memory cells may have been influenced by the lymphopenic environment in which they were generated. Overall these memory cells were more similar in response to altered peptide ligands than observed between WT and *Ptpn22*<sup>-/-</sup> naive and effector T cells.

These data suggested that in WT cells, Ptpn22 limits the generation of fully functional memory CD8 T cells in the context of lymphopenia but not strong Ag or inflammation. Consistent with this, fewer WT memory CD8 T cells were competent to produce IFN- $\gamma$  when they were induced by lymphopenia rather than by LmOva (Fig. 6g). On the other hand, *Ptpn22*<sup>-/-</sup> Ag- and HP-induced memory cells were equally effective in IFN- $\gamma$  production in response to both weak and strong peptides (Fig. 6h). Thus in the absence of Ptpn22 expression, HP is sufficient to induce the development of highly inflammatory

memory CD8 T cells, whereas in WT cells, this process needs initial stimulation with cognate Ag.

### Ptpn22 regulates LFA-1-dependent adhesion

Previously, we showed that TCR stimulation of *Ptpn22*<sup>-/-</sup> effector T cells resulted in increased activation of the guanine nucleotide exchange factor Rap1, that links inside-out TCR stimulation to LFA-1 function<sup>11</sup>. We hypothesized that the increased sensitivity of naive and effector *Ptpn22*<sup>-/-</sup> OT-1 T cells to weak ligands may be associated with an enhanced ability to form stable LFA-1-dependent cell contacts. Using a flow cytometry-based assay we monitored conjugate formation between naive OT-1 T cells and peptide-loaded APCs. Neither WT nor *Ptpn22*<sup>-/-</sup> OT-1 cells formed high numbers of conjugates with irrelevant control peptide SIY-loaded APCs whereas at all time-points assessed, WT and *Ptpn22*<sup>-/-</sup> OT-1 T cells were equally efficient at forming conjugates with N4-loaded APCs (Fig. 7a). At later time-points (2-4.5 h) *Ptpn22*<sup>-/-</sup> OT-1 cells formed significantly more conjugates with T4 or G4-loaded APCs than WT cells (Fig. 7a). Conjugate formation with peptide-loaded APCs was blocked by LFA-1 mAb, showing that the integrin is central to this interaction (Fig. 7a). To confirm that the higher conjugate stability was functionally relevant, we disrupted conjugates at different times following stimulation by addition of blocking LFA-1 Abs. LFA-1 blockade following 30-60 minutes of stimulation had a more profound impact on the responsiveness of *Ptpn22*<sup>-/-</sup> than WT OT-1 cells to G4 peptide stimulation, while not affecting the response of either genotype to strong N4 stimulation (Fig. 7b).

We assessed whether Ptpn22 influenced the activity of LFA-1 in CTL as well as in naive T cells, by monitoring the adhesion of WT and *Ptpn22*<sup>-/-</sup> OT-1 CTLs to ICAM-1 under conditions of flow. We obtained approximately 30% more adherent *Ptpn22*<sup>-/-</sup> T cells than WT cells under these conditions (Fig. 7c). These data indicate that Ptpn22 regulates LFA-1-dependent adhesion in a manner that is important for limiting the formation of conjugates between both naive and effector T cells with APCs presenting weak and/or self-antigens; the function of Ptpn22 in the WT animal is therefore to limit these responses while not impairing robust responses to strong agonist Ags.

### Discussion

The ability of T cells to discriminate low versus high affinity interactions is critical for the induction of protective immunity and the maintenance of self-tolerance. We show here that Ptpn22 acts to limit naive and effector T cell activation and the development of memory T cells in response to very weak and self-Ags. Early naive OT-1 T cell responses to weak agonist ligands were enhanced in the absence of Ptpn22 whereas responses to strong agonist peptides were indistinguishable to those of WT cells, as shown previously following anti-CD3/28 stimulation<sup>10-12</sup>. Thus Ptpn22 is a critical regulator of TCR ligand discrimination, permitting T cell activation by cognate Ags whereas restraining potentially damaging inflammatory responses to weaker ligands, which may include autoantigens.

In contrast to early responses such as Ras/Erk activation, cell growth and glucose uptake, later proliferative responses of *Ptpn22*<sup>-/-</sup> T cells in response to stimulation with peptides of



all affinities are enhanced. Therefore, in addition to a role in initial TCR activation, where it primarily acts as a break on responses to weak agonists, Ptpn22 plays a more general role in tempering expansion following activation. This latter role is coincident with upregulated expression of the protein between naive and effector T cells.

We provide evidence that regulation of the inside-out signaling pathway by Ptpn22 is important for ligand discrimination, as the ability of *Ptpn22*<sup>-/-</sup> T cells to form LFA-1-dependent conjugates with APCs pulsed with low affinity peptide was enhanced. Ptpn22 negatively regulates T cell activation, at least in part, by dephosphorylating critical tyrosine residues in TCR proximal kinases such as Lck and ZAP70<sup>33</sup> that, in turn, limits TCR-induced Rap1 activation and subsequent “inside-out” signaling to LFA-1<sup>11</sup>. Elevated Rap1 activity has previously been shown to enhance T cell activation and proliferation<sup>34</sup>. We show elevated conjugate formation by naive Ptpn22-deficient T cells directly correlates with increased responses to weak ligands influencing downstream expression of the TFs c-Myc, T-bet and IRF4.

Recently IRF4 was shown to be an important “rheostat” of TCR affinity, limiting the response of OT-1 T cells to weak agonists<sup>28</sup>. Consistent with this, up-regulation of IRF4 and downstream metabolic and effector cell function is elevated in response to weak agonists in *Ptpn22*<sup>-/-</sup> mice. Conversely, *Ptpn22*<sup>-/-</sup> mice show elevated Eomes expression in response to the stronger ligands that might favour production of long-lived memory cells. Our data fit with a model whereby, in WT cells, Ptpn22 limits T cell responses to weak agonists by restraining TCR and inside-out signaling pathways, thereby reducing up-regulation of critical TFs such as IRF4 and restraining effector cell differentiation.

T cell activation to weak antigens needs to be restrained particularly in conditions of lymphopenia as HP is associated with development of autoimmunity<sup>21</sup>. Secondary autoimmunity in relapsing-remitting multiple sclerosis patients following leukocyte depletion therapy using alemtuzumab<sup>35,36</sup> was shown to be a consequence of HP-induced T cell expansion<sup>6</sup>. Many autoimmune susceptibility genes identified in GWAS studies are involved in T cell regulation<sup>37</sup> and can increase the risk of lymphopenia-induced autoimmunity<sup>5,7</sup>. The *PTPN22* R619W variant is a risk allele for the development of several autoimmune diseases<sup>10</sup>, although the mechanism behind this predisposition is unknown. Mouse studies showed that homozygous expression of the variant *Ptpn22* allele resulted in a similar, albeit slightly milder, phenotype than Ptpn22-deficiency<sup>13,14</sup> and was sufficient for autoimmunity to develop spontaneously in an autoimmune-prone genetic background<sup>13</sup>. Our data show that Ptpn22 limits both the expansion of T cells and restrains the gain of pro-inflammatory function under HP conditions. It is possible that expression of disease-associated *PTPN22* alleles in the context of transient or chronic lymphopenia in human patients might increase the probability of autoimmune processes developing.

WT and *Ptpn22*<sup>-/-</sup> memory T cells induced by high affinity Ag during infection were similar in their ability to produce pro-inflammatory cytokines. Thus, Ptpn22 function is important to restrain the development of inflammatory memory cells in response to HP without markedly impeding their development during infection. Ptpn22 was previously thought to play a role in maintaining tolerance exclusively in effector T cells. The

importance of this role is emphasized by the finding that a self-peptide derived from  $\beta$ -catenin is sufficient to induce high levels of inflammatory cytokine production in *Ptpn22*<sup>-/-</sup> but not WT CTLs. Therefore, low level expression of Ptpn22 in naive T cells is sufficient and necessary to limit TCR activation in response to partial and weak agonists, whereas high Ptpn22 expression in effector cells is required to prevent highly sensitive effector T cell responses to bona fide self-Ag.

A related phosphatase, Ptpn2, was recently described to restrain HP in mouse T cells<sup>38</sup>, and regulate responses to low affinity peptides<sup>39</sup>. Given that both Ptpn2 and Ptpn22 target proximal signaling molecules<sup>33,40</sup>, it is perhaps unsurprising that their absence in mice would have similar phenotypes. Moreover variants of both *PTPN2* and *PTPN22* have been identified in GWAS screens as being linked with the same autoimmune diseases<sup>41</sup>. Further study of the physiological roles of these regulatory proteins and their disease-associated variants are thus of fundamental importance to improve our understanding of the mechanisms of immune activation, tolerance and autoimmunity.

## Online methods

### Mice, cell transfers and Listeria infection

*Ptpn22* Exon1<sup>fl/fl</sup> × PC3-Cre (global *Ptpn22*<sup>-/-</sup>) mice backcrossed to the C57BL/6J background (n=10) have been described<sup>11</sup> and were crossed to a *Rag1*<sup>-/-</sup> OT-1 TCR transgenic background<sup>19</sup>. *Ptpn22* Exon1<sup>fl/fl</sup> mice were crossed with the distal Lck (dLck)-Cre strain<sup>17</sup>. *CD3ε*<sup>-/-</sup>, *Rag1*<sup>-/-</sup>, C57BL6/J, CD45.1 and CD45.2 mice were bred in house at the University of Edinburgh. In some experiments, recipient mice were sublethally irradiated prior to cell transfer. For cell transfers, 2.5-5 × 10<sup>5</sup> CD45 congenic WT and *Ptpn22*<sup>-/-</sup> OT-1 or sorted naive CD4<sup>+</sup> T cells were mixed 1:1 and injected into recipients i.v. In some experiments, mice were infected i.v. with 10<sup>6</sup> c.f.u. of an ActA attenuated strain of ova-expressing *Listeria monocytogenes*<sup>31</sup>, a kind gift of Prof. H. Shen. Age (7-12 weeks) and sex-matched mice were used in all experiments. Where stated, groups of mice were administered 300 µg IL-7R mAb (A7R34, in house hybridoma) intraperitoneally, every second day over the 14 d experimental time-course. For transfer experiments, at least 4 mice / group were used allowing the detection of differences in mean values >1.5 fold with a SD of <0.25, with a power of 0.8 ([www.stat.ubc.ca/~rollin/stats/ssize](http://www.stat.ubc.ca/~rollin/stats/ssize)). As WT and *Ptpn22*<sup>-/-</sup> cells were co-transferred to recipient mice, randomization of animals and blinding of the investigator was not performed. All procedures were approved under a project license granted by the UK Home Office and performed in accordance with the institutional and ethical guidelines of the University of Edinburgh.

### Flow cytometry and antibodies

The following conjugated Abs were used: CD4-phycoerythrin (PE), CD4-allophycocyanin (APC) (both clone RM4.5), CD8β-PE Cy7 (eBioH35-17.2), CD25-PE (PC61.5), CD27-PE Cy7 (LG.7F9), CD44 APC eFluor780 (IM7), CD62L-eFluor450, CD62L-PE (both MEL-14), CD69-PE (H1.2F3), CD71-fluorescein isothiocyanate (FITC) (R17217), CD98-PE (RL388), CD127-PE (A7R34), TCRαβ-FITC (H57-597), KLRG1-APC (2F1), CXCR3-Peridin chlorophyll protein (PerCP) Cy5.5 (CXCR3-173), T-bet-PE (4B10), Eomes Alexa-

Fluor 647 (Dan11mag), IRF4-eFluor 450 (3E4), Ki-67-FITC (SolA15), granzyme B-PE (NG2B), TNF-APC (MP6-XT22), GM-CSF-PE (MP1-22E9), perforin-FITC (eBioOMAK-D) (all eBioscience), CD4-FITC (RM4.5), CD5-APC (53-7.3), CD11a-FITC (2D7), CD132-PE (Cat. No. 554457) (all BD Biosciences), CD4-Pacific Blue (PB) (RM4.5), CD25-Alexa Fluor 488 (PC61.5), CD45.2-PE, CD45.2-PB (Both 104), CD69-APC (H1.2F3), CD73-APC (TY/11.8), CD127 Brilliant Violet 421 (A7R34), IFN- $\gamma$ -Alexa Fluor 488 (XMG1.2), TNF-PerCP Cy5.5 (MP6-XT22) (all BioLegend) and CD45.1 FITC (A20) (Abcam). Unconjugated phospho-ERK T202/Y204 (197G2), phospho-RSK T359/S363 (Cat No. 9344) and Myc rabbit (D84C12) Abs were from Cell Signaling Technologies and were counterstained with goat anti-rabbit-PE (Molecular Probes). Live/dead Aqua and Cell Tracer violet dyes and 2NBDG were from Life Technologies. For intracellular staining, cells were fixed in BD Phosflow Lyse/Fix Buffer 1 or eBioscience FoxP3 Fix/Permeabilisation Buffer prior to Ab staining in Permeabilization/Wash buffers. For conjugate formation assays, the method of Grebe and Potter was adapted<sup>42</sup>. Splenocytes from CD3 $\epsilon^{-/-}$  mice were labeled with 1  $\mu$ M carboxyfluorescein succinimidyl ester (Molecular Probes) then loaded with 10<sup>-6</sup> M N4, T4, G4 or SIY peptide for 2h at 37°C. Cell tracer violet-labeled OT-1 and CFSE-labeled peptide-loaded APC were mixed 1:1 in 20  $\mu$ l RPMI and conjugate formation assessed by flow cytometry at timepoints indicated in figures. Samples were acquired with a MACSQuant flow cytometer (Miltenyi) and analyzed with FlowJo software (Treestar). Naive CD44<sup>low</sup> CD25<sup>-</sup> CD4<sup>+</sup> T cells were sorted using a FACSAria sorter (BD).

### Cell culture and stimulation

LN T cells from WT and *Ptpn22*<sup>-/-</sup> were cultured in RPMI 1640 media (Invitrogen) supplemented with 10% FCS, L-glutamine, antibiotics and 50 $\mu$ M 2-mercaptoethanol. N4, T4, G4 and RTYTYEKL peptides (Peptide Synthetics) were added to culture media at concentrations stated in figure legends. For growth of CTLs, OT-1 cells were stimulated for 2d with 10<sup>-8</sup>M N4, washed, then expanded/differentiated in 20 ng/ml recombinant human IL-2 or mouse IL-15 (Peprotech) for a further 4 d. For cytokine recall responses, cells were re-stimulated in the presence of 2.5  $\mu$ g/ml brefeldin A (Sigma) for 4h, prior to fixation and intracellular staining. For analysis of glucose uptake, following 24h peptide stimulation, cells were incubated for 45 min with 10  $\mu$ M NBDG, then washed twice in PBS prior to fixation in 2% paraformaldehyde and FACS analysis. Relative glucose uptake was calculated as the mean fluorescence intensity of NBDG staining following stimulation, with background fluorescence subtracted.

### Adhesion under shear flow

Adhesion of effector CTLs was assessed as described by Matthews and colleagues<sup>43</sup>. Briefly, Ibidi VI0.4 m-slides were coated with 6 mg/mL ICAM-1 overnight at 4°C. Effector CD8 T cells at a density of 10<sup>6</sup> cells/mL in adhesion medium (RPMI with 0.1% BSA, 40 mM HEPES and 2 mM MgCl<sub>2</sub>) were injected into a flow system that used a silicone tubing loop connected to a Multi-phaser NE-1000 syringe pump (New Era Pump Systems Inc.). Cells were allowed to flow over the ICAM-1-coated plates at a continuous shear flow rate of 0.5 dynes / cm<sup>2</sup> for 10 mins. Cells were monitored by microscopy and the number of adherent cells in the field of view was determined at 1 min intervals by manual counting.

## Statistical analysis

Student's *t*-test (paired or unpaired, 2 tails) and ANOVA were performed using Prism software.

## Supplementary Material

Refer to Web version on PubMed Central for supplementary material.

## Acknowledgements

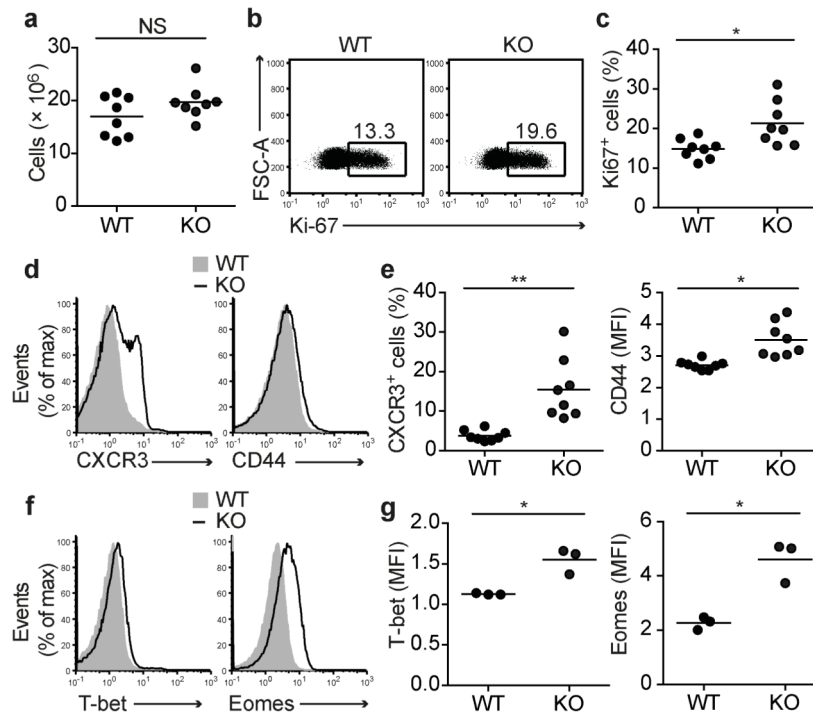
This study was funded by a Wellcome Trust senior investigator award (096669) to RZ, a Wellcome Trust Strategic Award for the Centre for Immunity, Infection and Evolution (095831) and VLM by BBSRC grant (801148). We are grateful for technical assistance from D. Wright and C. Garcia and to Dr. P. Travers for reading the manuscript.

## References

1. Polic B, Kunkel D, Scheffold A, Rajewsky K. How alpha beta T cells deal with induced TCR alpha ablation. *Proc Natl Acad Sci U S A*. 2001; 98:8744–8749. [PubMed: 11447257]
2. Goldrath AW, Bevan MJ. Low-affinity ligands for the TCR drive proliferation of mature CD8+ T cells in lymphopenic hosts. *Immunity*. 1999; 11:183–190.
3. Kieper WC, Jameson SC. Homeostatic expansion and phenotypic conversion of naive T cells in response to self peptide/MHC ligands. *Proc Natl Acad Sci U S A*. 1999; 96:13306–13311. [PubMed: 10557316]
4. Sprent J, Surh CD. Normal T cell homeostasis: the conversion of naive cells into memory-phenotype cells. *Nat Immunol*. 2011; 12:478–484.
5. Le Campion A, et al. Lymphopenia-induced spontaneous T-cell proliferation as a cofactor for autoimmune disease development. *Blood*. 2009; 114:1784–1793. [PubMed: 19561321]
6. Jones JL, et al. Human autoimmunity after lymphocyte depletion is caused by homeostatic T-cell proliferation. *Proc Natl Acad Sci U S A*. 2013; 110:20200–20205. [PubMed: 24282306]
7. King C, Ilic A, Koelsch K, Sarvetnick N. Homeostatic expansion of T cells during immune insufficiency generates autoimmunity. *Cell*. 2004; 117:265–277. [PubMed: 15084263]
8. Rhee I, Veillette A. Protein tyrosine phosphatases in lymphocyte activation and autoimmunity. *Nat Immunol*. 2012; 13:439–447. [PubMed: 22513334]
9. O'Shea JJ, McVicar DW, Bailey TL, Burns C, Smyth MJ. Activation of human peripheral blood T lymphocytes by pharmacological induction of protein-tyrosine phosphorylation. *Proc Natl Acad Sci U S A*. 1992; 89:10306–10310. [PubMed: 1279675]
10. Bottini N, Peterson EJ. Tyrosine Phosphatase PTPN22: Multifunctional Regulator of Immune Signaling, Development, and Disease. *Annu Rev Immunol*. 2014; 32:83–119. [PubMed: 24364806]
11. Brownlie RJ, et al. Lack of the phosphatase PTPN22 increases adhesion of murine regulatory T cells to improve their immunosuppressive function. *Sci Signal*. 2012; 5:ra87. [PubMed: 23193160]
12. Hasegawa K, et al. PEST domain-enriched tyrosine phosphatase (PEP) regulation of effector/memory T cells. *Science*. 2004; 303:685–689. [PubMed: 14752163]
13. Dai X, et al. A disease-associated PTPN22 variant promotes systemic autoimmunity in murine models. *J Clin Invest*. 2013; 123:2024–2036. [PubMed: 23619366]
14. Zhang J, et al. The autoimmune disease-associated PTPN22 variant promotes calpain-mediated Lyp/Pep degradation associated with lymphocyte and dendritic cell hyperresponsiveness. *Nat Genet*. 2011; 43:902–907. [PubMed: 21841778]
15. Wu DJ, et al. Autoimmunity-Associated LYP-W620 Does Not Impair Thymic Negative Selection of Autoreactive T Cells. *PLoS One*. 2014; 9:e86677.
16. Surh CD, Sprent J. Regulation of mature T cell homeostasis. *Semin Immunol*. 2005; 17:183–191. [PubMed: 15826823]

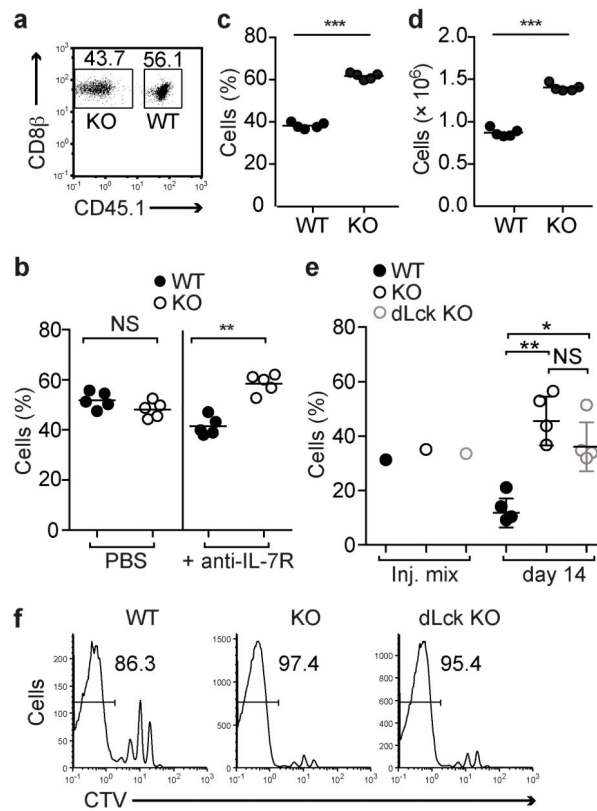
17. Zhang DJ, et al. Selective expression of the Cre recombinase in late-stage thymocytes using the distal promoter of the Lck gene. *J Immunol.* 2005; 174:6725–6731. [PubMed: 15905512]
18. Kieper WC, et al. Recent immune status determines the source of antigens that drive homeostatic T cell expansion. *J Immunol.* 2005; 174:3158–3163. [PubMed: 15749843]
19. Hogquist KA, et al. T cell receptor antagonist peptides induce positive selection. *Cell.* 1994; 76:17–27. [PubMed: 8287475]
20. Yachi PP, Ampudia J, Zal T, Gascoigne NR. Altered peptide ligands induce delayed CD8-T cell receptor interaction--a role for CD8 in distinguishing antigen quality. *Immunity.* 2006; 25:203–211. [PubMed: 16872849]
21. Daniels MA, et al. Thymic selection threshold defined by compartmentalization of Ras/MAPK signalling. *Nature.* 2006; 444:724–729. [PubMed: 17086201]
22. Enouz S, Carrie L, Merkler D, Bevan MJ, Zehn D. Autoreactive T cells bypass negative selection and respond to self-antigen stimulation during infection. *J Exp Med.* 2012; 209:1769–1779. [PubMed: 22987800]
23. D'Ambrosio D, Cantrell DA, Frati L, Santoni A, Testi R. Involvement of p21ras activation in T cell CD69 expression. *Eur J Immunol.* 1994; 24:616–620. [PubMed: 7907294]
24. Kaech SM, Cui W. Transcriptional control of effector and memory CD8+ T cell differentiation. *Nat Rev Immunol.* 2012; 12:749–761. [PubMed: 23080391]
25. Sullivan BM, Juedes A, Szabo SJ, von Herrath M, Glimcher LH. Antigen-driven effector CD8 T cell function regulated by T-bet. *Proc Natl Acad Sci U S A.* 2003; 100:15818–15823. [PubMed: 14673093]
26. Wang R, et al. The transcription factor Myc controls metabolic reprogramming upon T lymphocyte activation. *Immunity.* 2011; 35:871–882. [PubMed: 22195744]
27. Intlekofer AM, et al. Effector and memory CD8+ T cell fate coupled by T-bet and eomesodermin. *Nat Immunol.* 2005; 6:1236–1244. [PubMed: 16273099]
28. Man K, et al. The transcription factor IRF4 is essential for TCR affinity-mediated metabolic programming and clonal expansion of T cells. *Nat Immunol.* 2013; 14:1155–1165. [PubMed: 24056747]
29. Raczkowski F, et al. The transcription factor Interferon Regulatory Factor 4 is required for the generation of protective effector CD8+ T cells. *Proc Natl Acad Sci U S A.* 2013; 110:15019–15024. [PubMed: 23980171]
30. Yao S, et al. Interferon regulatory factor 4 sustains CD8(+) T cell expansion and effector differentiation. *Immunity.* 2013; 39:833–845. [PubMed: 24211184]
31. Foulds KE, et al. Cutting edge: CD4 and CD8 T cells are intrinsically different in their proliferative responses. *J Immunol.* 2002; 168:1528–1532. [PubMed: 11823476]
32. Santori FR, et al. Rare, structurally homologous self-peptides promote thymocyte positive selection. *Immunity.* 2002; 17:131–142. [PubMed: 12196285]
33. Wu J, et al. Identification of substrates of human protein-tyrosine phosphatase PTPN22. *J Biol Chem.* 2006; 281:11002–11010. [PubMed: 16461343]
34. Sebzda E, Bracke M, Tugal T, Hogg N, Cantrell DA. Rap1A positively regulates T cells via integrin activation rather than inhibiting lymphocyte signaling. *Nat Immunol.* 2002; 3:251–258. [PubMed: 11836528]
35. Cohen JA, et al. Alemtuzumab versus interferon beta 1a as first-line treatment for patients with relapsing-remitting multiple sclerosis: a randomised controlled phase 3 trial. *Lancet.* 2012; 380:1819–1828. [PubMed: 23122652]
36. Coles AJ, et al. Alemtuzumab for patients with relapsing multiple sclerosis after disease-modifying therapy: a randomised controlled phase 3 trial. *Lancet.* 2012; 380:1829–1839. [PubMed: 23122650]
37. Zhernakova A, van Diemen CC, Wijmenga C. Detecting shared pathogenesis from the shared genetics of immune-related diseases. *Nat Rev Genet.* 2009; 10:43–55. [PubMed: 19092835]
38. Wiede F, La Gruta NL, Tiganis T. PTPN2 attenuates T-cell lymphopenia-induced proliferation. *Nat Commun.* 2014; 5:3073. [PubMed: 24445916]

39. Wiede F, et al. T cell protein tyrosine phosphatase attenuates T cell signaling to maintain tolerance in mice. *J Clin Invest.* 2011; 121:4758–4774. [PubMed: 22080863]
40. Shields BJ, et al. TCPTP regulates SFK and STAT3 signaling and is lost in triple-negative breast cancers. *Mol Cell Biol.* 2013; 33:557–570. [PubMed: 23166300]
41. Zikherman J, Weiss A. Unraveling the functional implications of GWAS: how T cell protein tyrosine phosphatase drives autoimmune disease. *J Clin Invest.* 2011; 121:4618–4621. [PubMed: 22080861]
42. Grebe KM, Potter TA. Enumeration, phenotyping, and identification of activation events in conjugates between T cells and antigen-presenting cells by flow cytometry. *Sci STKE.* 2002; 2002:p114. [PubMed: 12223890]
43. Matthews SA, et al. Protein kinase D isoforms are dispensable for integrin-mediated lymphocyte adhesion and homing to lymphoid tissues. *Eur J Immunol.* 2012; 42:1316–1326. [PubMed: 22311617]



**Figure 1.**

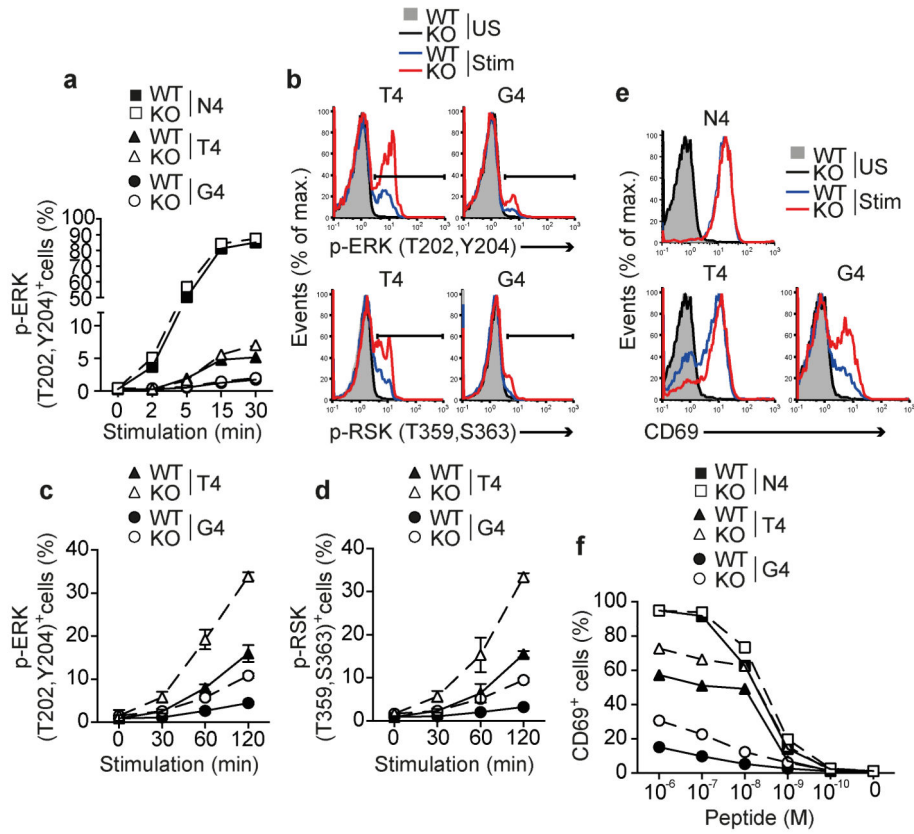
Ptpn22 limits basal activation of OT-1 T cells. (a) Quantification of the total numbers of CD8<sup>+</sup> T cells in LN of 7 wk old *Ptpn22*<sup>+/+</sup> (WT) and *Ptpn22*<sup>-/-</sup> (KO) *Rag1*<sup>-/-</sup> mice (n=8 mice/group). (b,c) Intracellular levels of Ki-67 *ex vivo*. Representative FACS dotplots (b) and graph (c) showing proportions of Ki-67<sup>+</sup> CD8<sup>+</sup> T cells (n=8 mice/group). (d,e) Surface expression of CXCR3 and CD44. Representative histograms (d) and graphs (e) showing expression of CXCR3 and CD44 on gated CD8<sup>+</sup> OT-1 T cells. (f,g) Basal expression of T-bet and Eomes. Representative flow cytometry histograms (f) and graphs (g) showing basal intracellular expression of T-bet and Eomes (n=3 mice/group, in 1 of 3 repeated experiments). In graphs, lines represent mean values and each dot represents the values from one mouse of each genotype. NS – not significant, \* - p<0.01, \*\* - p<0.001 by Students t-test.



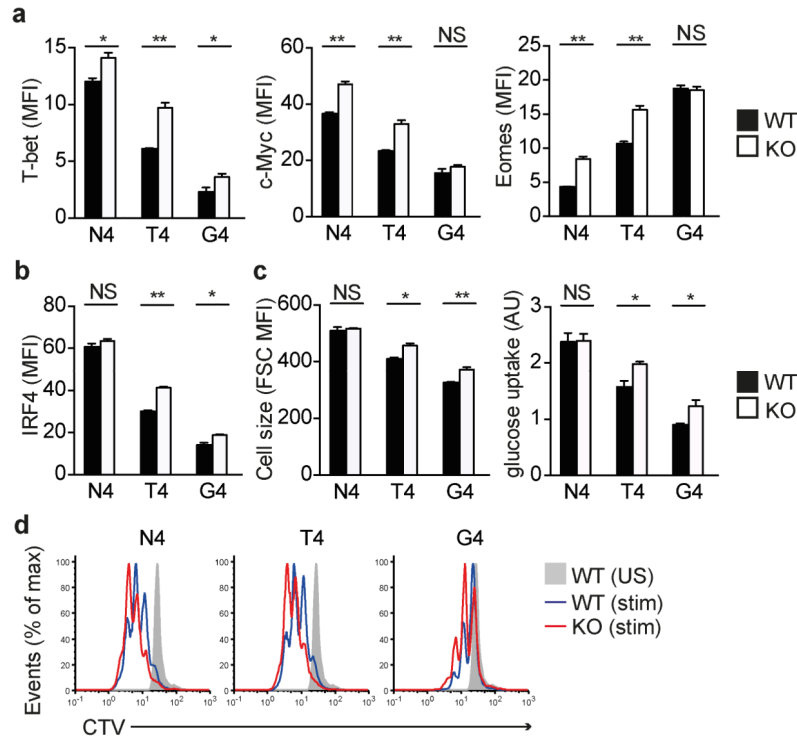
**Figure 2.**

Lymphopenia-induced proliferation is inhibited by *Ptpn22*. (**a-d**) WT CD45.1<sup>+</sup> and *Ptpn22*<sup>-/-</sup> CD45.2<sup>+</sup> OT-1 cells were mixed ~1:1 and transferred i.v. to *Rag1*<sup>-/-</sup> hosts. (**a**) Flow cytometry dotplot showing typical proportions of WT and *Ptpn22*<sup>-/-</sup> (KO) OT-1 cells injected. Proportions (**b**) of WT and *Ptpn22*<sup>-/-</sup> (KO) cells recovered 14 d post-transfer from LN and spleens of recipient mice treated with either PBS (left) or anti-IL-7R mAb (right) (n=5 mice/group). Proportions (**c**) and absolute cell numbers (**d**) of WT and *Ptpn22*<sup>-/-</sup> cells recovered from LN and spleens of recipient mice 30d post-transfer (n=5 mice/group). (**e,f**) CellTrace Violet (CTV)-labeled polyclonal naive CD4<sup>+</sup> T cells from WT CD45.1<sup>+</sup>, global *Ptpn22*<sup>-/-</sup> CD45.2<sup>+</sup>, or dLck-Cre × *Ptpn22*<sup>fl/fl</sup>-GFP<sup>+</sup> mice were mixed ~1:1:1 (injection mix – inj. mix) and transferred to irradiated CD45.1/CD45.2 F<sub>1</sub> recipients. (**e**) Proportions of cells recovered 14d post transfer from LN and spleens of recipient mice (n=4 mice/group). (**f**) Representative histograms show dilution of cell-tracer dye from d14 post-transfer cells recovered from recipient mice. Values in histograms represent proportion of cells in which CTV dye had been completely diluted. Data in all graphs represent one of at least two repeated experiments. Dots represent values from individual mice and lines represent means for each genotype. NS – not significant, \* p<0.05, \*\* p<0.01, \*\*\* p<0.001 by Student's *t*-test.

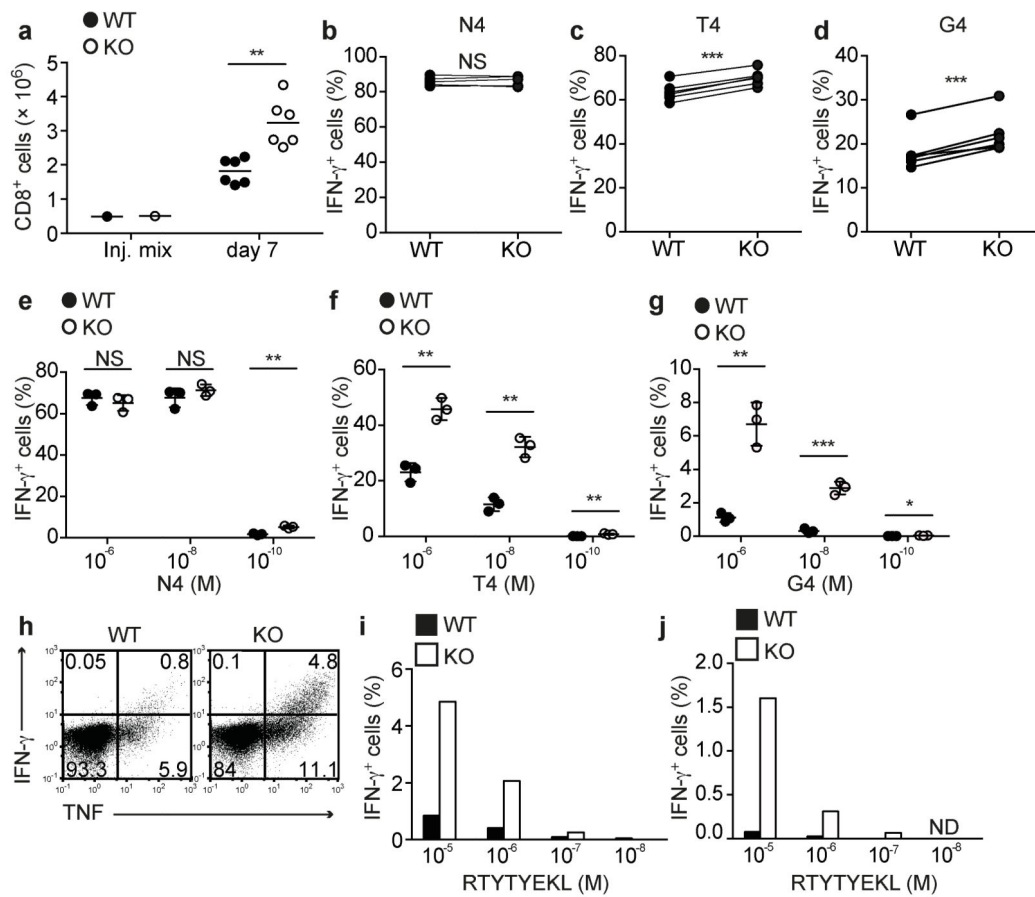


**Figure 3.**

*Ptpn22* limits weak agonist induced TCR triggering in naive T cells. Responses of WT and *Ptpn22*<sup>-/-</sup> (KO) OT-1 cells are indicated throughout. (a) Proportions of phospho-ERK<sup>+</sup> CD8 T cells following stimulation with 10<sup>-6</sup> M peptide for the time periods indicated. (b) Representative histograms showing intracellular staining for p-ERK and p-RSK following 2h stimulation with 10<sup>-6</sup> M T4 or G4 peptide. Time courses of ERK (c) and RSK (d) activation following T4 and G4 stimulation; symbols represent mean values and error bars SD (n=3 replicate samples). (e) Histograms showing surface CD69 expression under basal conditions (unstimulated – US) or following 4h stimulation (Stim) with 10<sup>-6</sup> M variant peptides. (f) Dose response curves of CD69 upregulation. For all graphs, data are representative of 1 of at least 3 repeated experiments.

**Figure 4.**

*Ptpn22* inhibits TCR-induced metabolic changes, transcription factor expression and proliferation. Protein expression of T-bet, Myc, eomesodermin (Eomes) (a) and IRF4 (b) expression following 24 h of stimulation of WT and *Ptpn22*<sup>-/-</sup> OT-1 cells with 10<sup>-6</sup> M variant ova-peptides as determined by flow cytometry analysis of the mean fluorescence intensity of staining (MFI). (c) Cell size (forward scatter [FSC] MFI) and relative glucose uptake (arbitrary units – AU) by OT-1 cells following 24h stimulation as determined by flow cytometry. (d) Representative histograms showing dilution of CellTrace Violet (CTV) dye after 48h of peptide stimulation (from 1 of 3 repeated experiments). WT and *Ptpn22*<sup>-/-</sup> genotype *Rag1*<sup>-/-</sup> OT-1 T cells were used as indicated throughout. In all barcharts, values represent means and error bars SD (n=3 replicate samples, from 1 of 4 repeated experiments). NS – not significant, \* p<0.01, \*\* p<0.001 by two-tailed unpaired Student's *t*-test.

**Figure 5.**

Ptpn22 restrains weak agonist-induced inflammatory cytokine production by effector CTLs. (a-d) Day 7 CTLs were generated *in vivo* by co-transfer of WT CD45.1<sup>+</sup> and *Ptpn22*<sup>-/-</sup> (KO) CD45.2<sup>+</sup> *Rag1*<sup>-/-</sup> OT-1 cells at a ~1:1 ratio to *Rag1*<sup>-/-</sup> hosts followed by LmOva infection (n=6 mice/group). (a) Absolute numbers of recovered CTLs from recipient mice at d7 post-infection. Amounts of intracellular IFN- $\gamma$  production by *ex vivo* CTLs following 4h re-stimulation with  $10^{-6}$  M N4 (b), T4 (c) or G4 (d) peptides. Dots connected by lines represent paired WT and *Ptpn22*<sup>-/-</sup> CTL samples retrieved from the same recipient mouse. (e-j) CTLs were generated *in vitro* by N4 peptide stimulation followed by expansion and differentiation in IL-2 or IL-15. Dose responses of IL-2-differentiated WT and KO CTLs following 4h re-stimulation with N4 (e), T4 (f) or G4 (g) peptides (n=3 mice/group). Lines represent mean values and dots represent CTLs generated from individual mice of each genotype. NS – not significant, \* p<0.05, \*\* p<0.01, \*\*\* p<0.001 by two-tailed unpaired Student's *t*-test. (h) Representative dotplot showing IFN- $\gamma$  and TNF production following re-stimulation of IL-2 generated CTLs with  $10^{-5}$  M RTYTYEKL. Dose response of RTYTYEKL-induced IFN- $\gamma$  production by IL-2-generated (i) and IL-15-generated (j) CTLs; data are from 1 of 3 repeated experiments. ND – not detectable.

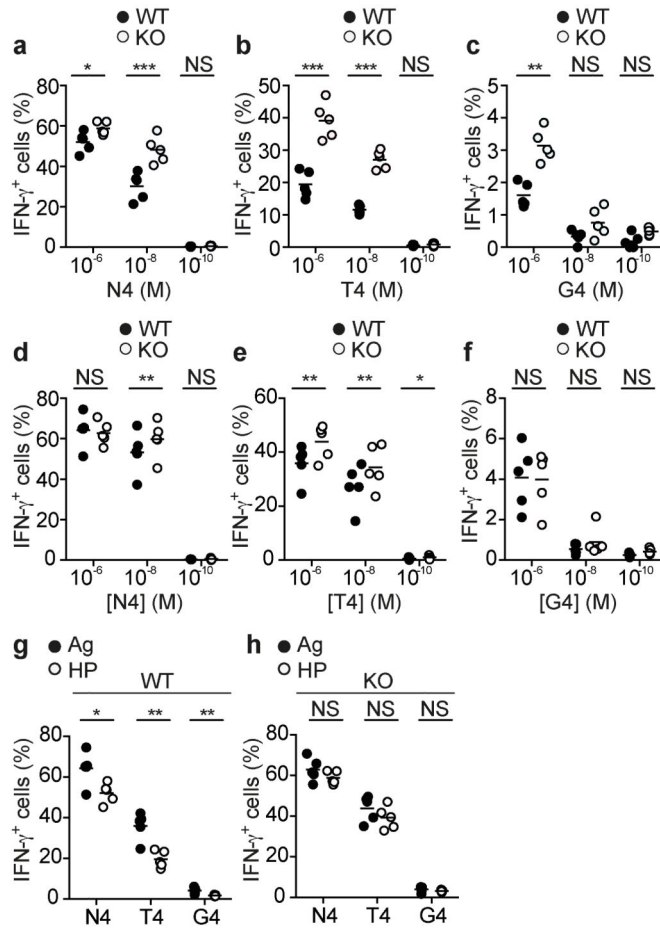


**Figure 6.**

Ptpn22 limits the pro-inflammatory capacity of HP-induced memory T cells. WT and *Ptpn22*<sup>-/-</sup> (KO) HP-induced (a-c) or LmOva-induced (d-f) *Rag1*<sup>-/-</sup> OT-1 memory T cells were recovered from *Rag1*<sup>-/-</sup> recipients 30d post-transfer. Dose response of HP-induced and Ag-induced memory cells IFN- $\gamma$  production following re-stimulation with N4 (a,d), T4 (b,e) or G4 (c,f). Comparison of functional capacity of WT (g) or KO (h) Ag- and HP-induced memory cells. In all cases, lines represent means and dots values from individual mice. All data are representative of 1 of 2 repeated experiments (n=5 mice/group). NS – not significant, \* p<0.05, \*\* p<0.01, \*\*\* p<0.001 by paired (a-f) or unpaired (g,h) Student's *t*-test.

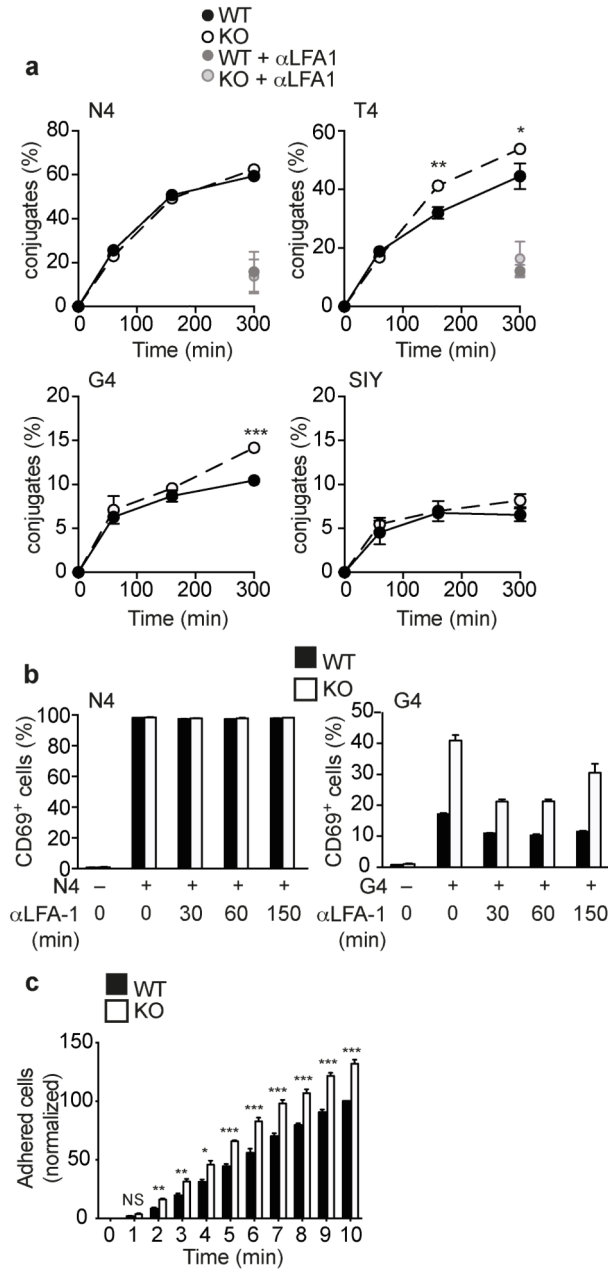


**Figure 7.** Elevated LFA-1-dependent adhesion and conjugate formation by *Ptpn22*<sup>-/-</sup> T cells is important for the increased responses to weak Ags. **(a)** Flow cytometry analyses assessing conjugate formation of naive WT and *Ptpn22*<sup>-/-</sup> *Rag1*<sup>-/-</sup> OT-1 T cells with N4, T4, G4 or SIY-loaded APCs. Error bars represent SD (n=3 replicate samples) and data are representative of 3 repeated experiments. **(b)** Blocking LFA-1 mAbs were added at various time points, as indicated, following N4 or G4 peptide stimulation of naive WT and *Ptpn22*<sup>-/-</sup> OT-1 cells and CD69 upregulation measured at 4 h. Data shown are means  $\pm$  SD (n=3 replicate samples) from one of two repeated experiments. **(c)** Adhesion of WT and KO effector CTL to ICAM-1 under flow. Error bars represent SD (n=4 mice/group) and data are

representative of 2 repeated experiments. NS – not significant, \*  $p < 0.05$ , \*\*  $p < 0.01$ , \*\*\*  $p < 0.001$  by Student's *t*-test (**a**) or ANOVA (**c**).